JOURNAL OF MATERIALS SCIENCE 30 (1995) 5522–5530

Tensile dilatometry of injection-moulded HDPE/PA6 blends

S. FELLAHI, B. D. FAVIS, B. FISA
Centre de recherche appliquée sur les polymères (CRASP), Ecole Polytechnique de Montréal, P.O. Box 6079, Station "Centre-ville", Montréal, Québec, Canada, H3C 3A7

In order to understand the mechanism of deformation of injection-moulded HDPE/PA6 (25 vol% /75 vol%) blends both with and without compatibilizer, the volume change has been monitored using tensile dilatometry. Dog-bone specimens were either directly moulded or cut from rectangular plaques. Both neat materials and their blends were tested. For the directly moulded dog-bone specimen, a pure shear yielding mechanism was observed for all materials tested, i.e. PA6, HDPE, and their blends in the same proportion as above. In the case of a deformable minor phase (HDPE), the dispersed phase appeared to bear its share of stress and the flow-induced orientation mimics the effect of interfacial modification. This was not the case of a rigid minor phase (glass beads) at the same concentration; the effect of surface treatment changed the mechanism of deformation from mixed mode cavitation shear yielding (45%) to almost pure shear yielding (85%). Machined specimens made of neat PA6 and HDPE deformed through pure shear yielding. The addition of 25 vol% HDPE to PA6 resulted in a mixed mode cavitation (55%)/shear yielding mechanism of deformation in the transverse direction, while in the longitudinal case, the mechanism which prevailed was almost pure shear yielding (80%). This can be attributed to the flow-induced orientation as above. When adding 10% (based on the weight of the dispersed phase) of an ionomer as a compatibilizer, the blend deformed via shear yielding (85%) and in the longitudinal direction both compatibilized and non-compatibilized blends display similar behaviour. Varying the specimen thickness by changing the mould cavity, led to a significant variation in the dilatational behaviour. Dilatometric behaviour is shown to be closely related to the morphology generated as a result of flow-induced orientation. The skin/core ratio, which is an indication of the proportion of the oriented dispersed phase to the non-oriented one, plays a key role in influencing the mechanism of deformation involved.

1. Introduction

Polymer blends represent an area of growing interest to both scientific and industrial communities. These materials are physical blends of two or more polymers most often compatibilized through the introduction of a third agent or developed *in situ* through reactive processing [1–4].

In order to assess the mechanical performance in tension, it is standard procedure to rely on the usual stress–strain curve to obtain the stress at break and yield, the elongation at break and yield, the modulus, and Poisson's ratio. However, through the combined use of longitudinal and transverse extensometers much more information can be obtained. In the latter case the volume strain of the sample can be monitored and subsequently related to the various processes of deformation which may take place during the course of the experiment.

Injection-moulded parts are known to exhibit a three-layer structure: skin/subskin/core. Depending on the thickness of the part, the size of each layer may vary due to orientation, cooling and/or crystallization considerations [5, 6]. This is expected to have a profound effect on the mechanism of deformation in such systems.

Volume strain can be a useful indicator of the various processes which may occur during the course of the usual stress–strain experiment. Prior to yielding, there is primarily an elastic volume dilatation, normally expressed as the Poisson's ratio. After yielding, the volume behaviour reflects the relative extent of phenomena which do not display any volume change (shear yielding, shear-band deformation and cold drawing), as compared to cavitational phenomena (crazing, microvoiding). In the literature, different methods have been developed to study dilatational phenomena: (1) liquid displacement dilatometer [7–11], (2) the use of two or three extensometers [12–16], (3) the use of strain gauges [17].

The dilatometry technique was initially developed to obtain information on deformational mechanisms [7, 10–16, 18–21]. Bucknall and Clayton [12] were

0022–2461

the first to introduce this approach, to evaluate quantitatively, the deformation mechanism responsible for toughening. This technique was used to study craze formation in rubber-modified plastics during a creep experiment. The rate of volume change can be related directly to the rate of crazing. Bucknall and Clayton [22] applied this technique to compression-moulded HIPS during a creep test. Three deformation steps were observed: (1) an instantaneous dilatation attributed to an elastic response, (2) a slow dilatation, (3) a rapid dilatation. Steps 2 and 3 are attributed to crazing. In a recent paper, Naqui and Robinson [16] applied tensile dilatometry to polymethylmethacrylate (PMMA) and talc-filled polypropylene (PP). The engineering constants (tensile modulus and lateral contraction ratio) were measured and found to be viscoelastic. The volume strain response revealed a significant cavitation-type mechanism in the case of talc-filled PP, whereas PMMA showed a shear yielding mechanism. The volume strain was found to be directly related to the bulk modulus for these materials. The authors suggest a new method of presenting the results: volume strain versus stress.

Other authors have used tensile dilatometry to assess interfacial bonding in multiphase systems [7, 11, 23–25]. The technique has been applied to polystyrene (PS)/low-density polyethylene (LDPE) blends by Coumans *et al.* [7] to measure the sample volume change. It was found that Poisson's ratio was highly dependent on the presence of the compatibilizer. The authors also reported that shear banding increases with the level of compatibilizer.

The volume change of injection- and compression-moulded high-density polyethylene (HDPE)/polystyrene (PS) and (HDPE/polyether copolymers (PEC))/PS compatibilized with various amounts of a triblock copolymer (SEBS) based on styrene–butadiene was studied during uniaxial mechanical straining [11]. A reduced volume dilatation on adding SEBS, was observed, indicating better interfacial adhesion between the components of the first blend. The dilatational behaviour of the second blend was substantially less, suggesting more effective compatibilization. Microscopy results confirmed the above findings by showing the existence of good interfacial adhesion. Compression-moulded samples behaved differently, and these differences were attributed to morphological phenomena. In some cases, the authors reported that the volume dilatation peaks at the yield stress, but decreases after yielding as a result of reduced load on the sample.

Despite a certain body of literature on the subject of tensile dilatometry, no detailed work has been undertaken to elucidate the mechanism of deformation involved in injection moulded parts with variable geometry. This lack of information becomes even more crucial when it comes to multiphase systems in general and polymer blends in particular. It was therefore the aim of this work to consider the use of tensile dilatometry to investigate the process of deformation involved in injection-moulded HDPE/PA-6 and glass beads-filled PA-6. The role of interfacial modification on both systems in affecting the mechanism of deformation will also be shown. In addition, the influence of the geometry of the mould cavity to emphasize molecular and dispersed phase orientation and its influence on the deformation mechanism, will also be considered.

2. Experimental procedure

2.1. Materials

The polyamide-6 (PA-6) is a Zytel 211 from E.I. Dupont Inc. with a number average molecular weight, $M_n = 25\,000\ g\,mol^{-1}$. A high-density polyethylene from Dow Chemical Canada (Dow 06153C) having a melt flow index of 6.3 g/10 min, $M_n = 20\,200\ g\,mol^{-1}$, and $M_w = 81\,300\ g\,mol^{-1}$ was selected as a minor phase. The compatibilizing agent having $M_n = 25\,000\ g\,mol^{-1}$ is an ionomer (Surlyn 9020, Dupont Canada Inc.) terpolymer consisting of 80% polyethylene and 20% mixture of methacrylic acid and isobutyl acrylate. The methacrylic acid is 70% zinc neutralized. The polyethylene is stabilized with 0.2% antioxidant (Irganox 1010 of Ciba Geigy). Glass beads (untreated and silane treated), obtained from Potters Ballotini, were used as fillers in complementary experiments. The average bead diameter was about 45 μm.

2.2. Compounding

The first operation consisted in mixing the polyethylene with 0.2 wt % antioxidant in a single-screw extruder. Then, using a twin-screw extruder, 10 vol % ionomer (I) were admixed to the stabilized PE. Finally, 25 vol % polyethylene (PE) with or without compatibilizer, or 25 vol % glass beads, were incorporated into polyamide-6 (PA6). Prior to a typical mixing operation, the sample mixture was dried overnight at 90 °C under vacuum to minimize hydrolytic degradation of the polyamide during processing. The polymer blending was carried out on a ZSK-30 (Werner-Pfleiderer) intermeshing, co-rotating twin-screw extruder with a screw length to diameter ratio, L/D, of 40. Feeding was performed under nitrogen and vacuum was applied in the decompression zone. The blending conditions can be found elsewhere [26, 27]. Neat PA6 has been twin-screw extruded to give it the same thermal history as the PA6 in the blends.

2.3. Injection moulding

The injection-moulding machine used was a Battenfeld type BA-C 750/300, with a clamping force of 80 ton. Two experimental moulds, both with interchangeable cavities were employed. A rectangular plaque (127 mm × 76 mm × 2, 4 and 6 mm cavity depth) is used. It is provided with a 2 mm deep flash gate fed with a trapezoidal duct having a section varying from 30–50 mm^2. Tensile test bars were cut at different locations and termed as type II specimens (Fig. 1). Directly moulded 3 mm dog-bone tensile bars (type I in Fig. 1) were produced. As-received neat PA6, HDPE, as well as the prepared compounds were injection moulded. The moulding conditions were the same

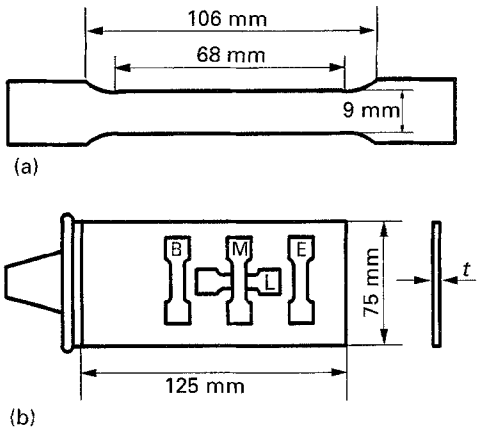

Figure 1 Mould cavities used in this work. (a) Type I, moulded tensile specimens. (b) Type II, rectangular plaque with location at which samples were machined.

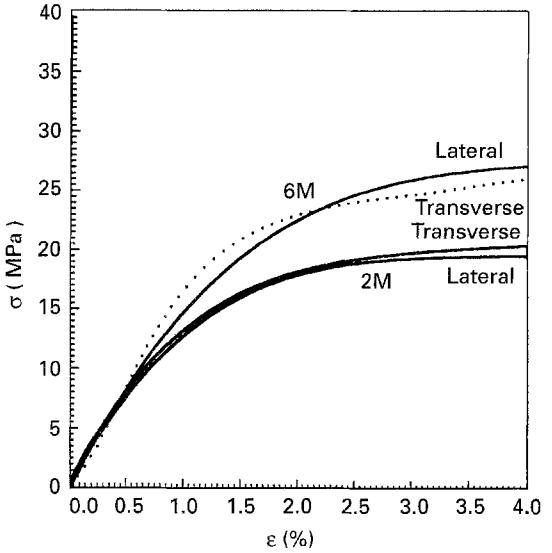

Figure 2 Stress versus elongation curves showing the behaviour in both the lateral and transverse directions. Two samples, type II 2 and 6 mm, 75% PA/25% HDPE (non-compatibilized) are shown.

for both types and have been reported elsewhere [26, 27].

2.4. Tensile testing

Prior to testing, all samples were conditioned at 23 °C and 50% R.H. for several days. The ASTM D638 standard was followed. Type I samples were tested directly while a special dog-bone shaped sample was designed to make the best use of the type II plaques. Samples were machined transversally at different positions (B, M and E) and longitudinally (L) from plaques as illustrated in Fig. 1. A universal tensile machine was used with a crosshead speed of 5 mm min^{-1}, and 2.5 kN maximum load, to generate the stress–strain curves. For the latter case, an MTS extensometer (632.13C.20) with a 10 mm gauge length was used. The load and axial extension were recorded using a data acquisition software.

2.5. Tensile dilatometry

The tensile test was carried out according to ASTM D638. The volume change measurement was carried out during the tensile test using the above-mentioned axial extensometer, and an Instron transverse extensometer model 2640.007. It is assumed that the deformation in the thickness is equal to that in the width [24]. Both extensometers were attached to the specimen. Lateral and axial extension were recorded simultaneously on a PC using a data acquisition software. From the axial strain, ε_a, and the transverse strain, ε_T, one can compute the volume strain, $\Delta V/V_0$, as

$$\Delta V/V_0 = (1 + \varepsilon_a)(1 + \varepsilon_T)^2 - 1 \quad (1)$$

and Poisson's ratio as

$$\nu = -\frac{\varepsilon_T}{\varepsilon_a} \quad (2)$$

Note that ε_T assumes a negative value. In addition to that, in a plot of $\Delta V/V_0$ versus ε_a, a post-yield slope of 1 indicates that the mechanism of deformation is due to pure crazing, while for a nil post-yield slope, the mechanism which prevails is pure shear yielding with no volume change. A mixed mode mechanism of deformation will situate itself between the two extremes.

In order to verify that the transverse and lateral elongations were the same, tests were carried out on the specimens considered to be the most anisotropic (non-compatibilized Type II 2 and 6 mm samples). The results of stress, σ, versus elongation, ε, for both samples in the lateral and transverse directions are shown in Fig. 2. It is quite clear that, within experimental error, the curves superimpose. In addition, for all samples studied, the deformation within the gauge length was homogeneous.

2.6. Scanning electron microscopy

The surfaces of samples which had been deformed up to 15% axial strain, were freeze fractured, coated with a layer of gold/palladium, and observed under a Jeol 820 scanning electron microscope at 10 kV.

3. Results and discussion

Most of the published literature concerning the mechanical properties of injection-moulded articles, reports the use of a directly moulded dog-bone type specimen. In actual applications, however, a plaque-type mould is more representative. For this reason a comparison was carried out between the two specimen types. Another advantage of using plaques is that the mould thickness can be varied hence allowing one to modify the skin/core ratio and evaluate the influence of orientation. Plaque specimens also allow for the measurement of the transverse properties.

3.1. Directly moulded dog-bone specimens (type I)

3.1.1. Influence of a rigid or deformable minor phase

3.1.1.1. Neat polymers. The behaviour of PA-6 can be described as follows: in the range of strains studied

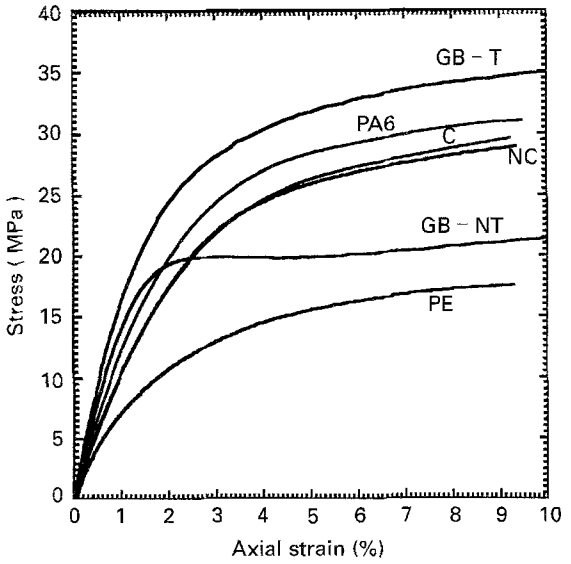

Figure 3 Stress versus strain curves for type I specimens for different materials: PA-6, HDPE, GB-T, treated glass bead-filled PA-6; GB-NT, untreated glass bead-filled PA-6; C, NC, with and without compatibilizer, respectively, for HDPE/PA-6 blends.

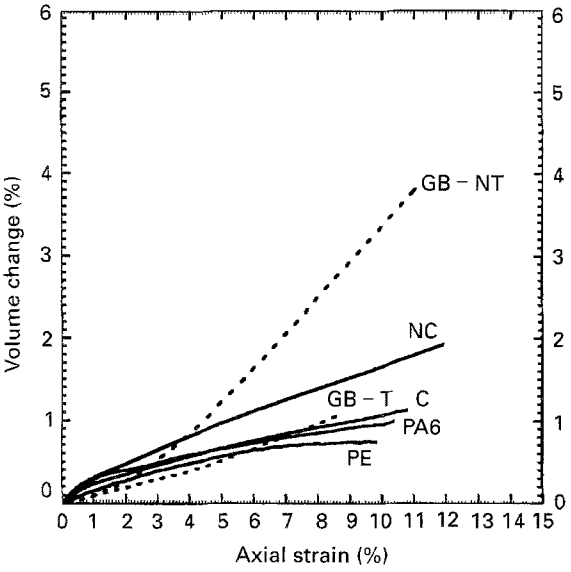

Figure 4 Volume change versus axial strain of type I specimen. Same notation as in Fig. 2.

(< 10%) the PA-6 stress–strain curve has not reached a maximum (Fig. 3). However, during the first elastic stage which is observed at (0%–1%) the Poisson's ratio is 0.48. It is worth noting that the volume change versus axial deformation is almost linear after the initial increase due to the elastic effect, as shown in Fig. 4. The ΔV is essentially negligible, and the mechanism of deformation which prevails is shear yielding (post-yield slope = 0.06 as shown in Table I), as already reported in the literature [24].

With respect to the behaviour of HDPE, there is a ΔV increase of approximately 0.5% up to the yield point due to elastic deformation, and beyond that no volume change is observed (Fig. 4). This indicates a shear yielding process of deformation (Table I).

TABLE I Post-yield and Poisson's ratio, v, at 0.5% axial deformation. Directly moulded (Type I) specimens. C, NC, with and without compatibilizer, respectively.

Materials	Slope	Poisson's ratio
PA-6	0.06	0.47
HDPE	0.04	0.42
NC	0.16	0.45
C	0.10	0.465
25-NT[a]	0.45	0.46
25-T[a]	0.15	0.47

[a] 25 vol % glass bead-filled PA-6, (T) treated and (NT) not treated.

3.1.1.2. Blend with rigid dispersed phase. The comparison of various materials used in this work at small strains provides a very valuable insight into their behaviour as shown in Fig. 3. To draw the stress–strain curves, the strain was assumed to be identical to the extensometer displacement. Fig. 3 shows the stress–strain curves of both blends, of the polyamide-6 filled with 25 vol % glass beads (untreated and silane treated), as well as those of both neat starting materials (PE and PA6). In the polyamide containing poorly adhering glass beads (curve GB-NT), the stress reaches a maximum at about 2% strain. The yield stress of this material is approximately equal to that of the unfilled polyamide, reduced by the factor representing the area occupied by glass beads. This confirms work in a previous study where it was shown that at yield essentially all the glass beads debonded from the matrix [28]. With untreated glass beads and with the non-compatibilized blend (NC) the interfacial debonding begins at about the same level of strain, i.e. 1.5%. However, the material filled with untreated beads dilates at a significantly faster rate (0.45 slope) than the uncompatibilized blend (0.16 slope) as shown in Fig. 4 and Table I. SEM observations of the untreated glass bead-filled PA-6 shown in Fig. 5a and taken after mechanical testing, clearly show debonding and significant cavitation.

3.1.1.3. Blend with deformable dispersed phase. When 25 vol % HDPE is added to PA6 a slight decrease in the tensile stress (Fig. 3) is recorded. This decrease has been reported in the literature [29] and is attributed to the poor interface, but it is apparent that the PE minor phase appears to bear its share of stress because the untreated HDPE/PA-6 blend displays similar behaviour to neat PA-6. In addition, as seen in Fig. 4 for the untreated blend, an increase in ΔV with axial strain is observed. The dependence of ΔV is linear and reaches 2% at 12% axial strain. Some stress whitening was observed on the specimen. The mechanism which prevails is predominantly shear yielding (slope 0.16). When compared to neat PA6, with a post-yield slope of 0.06 the difference is very small (Table I). SEM observations for the untreated HDPE/PA-6 blend clearly show extensive dispersed phase orientation in the sample. Fig. 6 shows differences between the core and the subskin region. In fact, detailed study of the skin, subskin/core ratio shows it to be 30/1. These

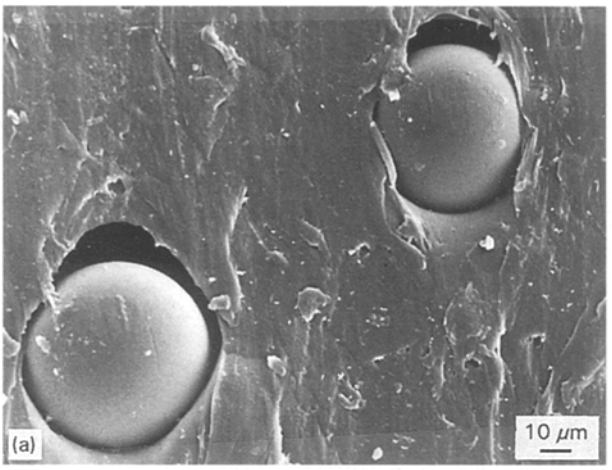

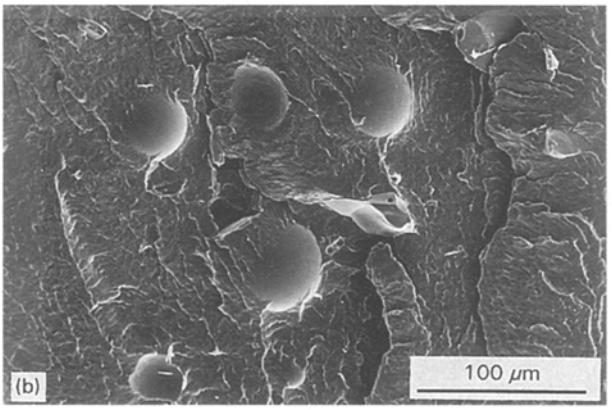

Figure 5 Micrograph of fracture surface of type I glass bead-filled PA-6 (transverse to flow view), (a) untreated, (b) treated glass beads.

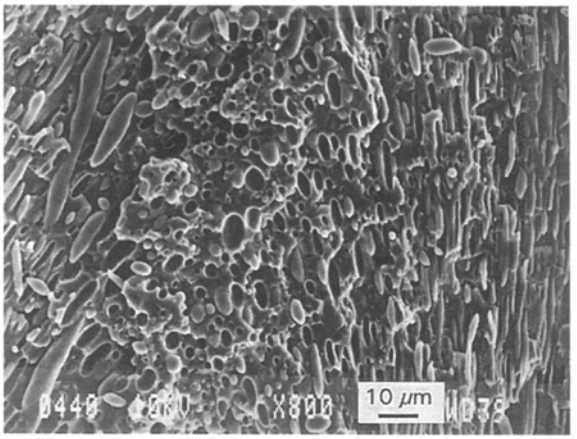

Figure 6 Micrograph of fracture surface of type I non-compatibilized blend (transverse to flow view).

samples, therefore, are essentially highly oriented except for a narrow portion in the middle.

In summary, PA-6 filled with a rigid dispersed phase shows significant differences in both the stress–strain and dilatometric behaviour (increased cavitational phenomena) when compared with neat PA-6. With untreated glass beads as the minor phase, there is no chance for them to deform. Under loading, glass beads debond, leading to loss of strength and formation of voids or cavitation. PA-6 with a deformable HDPE minor phase, however, displays much less variation with respect to neat PA-6. Morphological observations demonstrate significant cavitation at the interface for untreated glass beads filled PA-6 (Fig. 5a) and significant orientation of the dispersed phase in HDPE/PA-6 blends with a skin/core ratio equal to 30/1 (Fig. 6). These results strongly indicate that dispersed phase orientation plays a predominant role in determining the mechanism of deformation (cavitation/shear yielding) for non-compatibilized systems. This supposition will be examined in more detail later in the paper.

3.1.2. Effect of interfacial modification

3.1.2.1. Blend with a rigid dispersed phase. The stress–strain curve of treated glass-bead filled PA-6 is shown in Fig. 3. When glass beads are treated with silanes, little or no debonding takes place in the range of strains considered [28], and the stress borne by the material at a given strain exceeds that of the neat PA6 (curve GB-T). The rate of volume change in this system is very slow (slope 0.15) indicating the good interfacial adhesion achieved through the use of silanes (Figs 3 and 5). Fig. 5 illustrates the effect of surface treatment. While the matrix debonded from untreated beads creating elongated cavities (Fig. 5a), the treated beads appear to be solidly anchored to the matrix (Fig. 5b). This results in a more compact structure with no chance of debonding and the mechanism of deformation which prevails is shear yielding (Fig. 4 and Table I).

3.1.2.2. Blend with a deformable dispersed phase. As shown in Fig. 3, the addition of a compatibilizer to the HDPE/PA-6 blend results in tensile properties very similar to the non-compatibilized case in the range of strains considered. The compatibilizer also has little effect on the dilatometric behaviour as observed in Fig. 4 and Table I. The volume strain recorded with the compatibilized blend (post-yield slope 0.10) is small. In fact it is very similar to that recorded for both that of the neat polymer (post-yield slope 0.06) as well as the polymer filled with treated glass beads (post-yield slope 0.15).

This result shows that in both blends tested under these conditions the dispersed phase bears its share of stress. This may seem surprising in view of the data obtained by the tensile dilatometry (Fig. 4). Despite some debonding, the dispersed phase of the non-compatibilized blend can bear the same load as in its compatibilized counterpart. An elongated dispersed phase particle of variable cross-section and shape trapped in the matrix appears to deform along with the matrix in spite of the lack of interfacial adhesion. It is apparent from these results that the influence of flow-induced orientation mimics the effect of compatibilization.

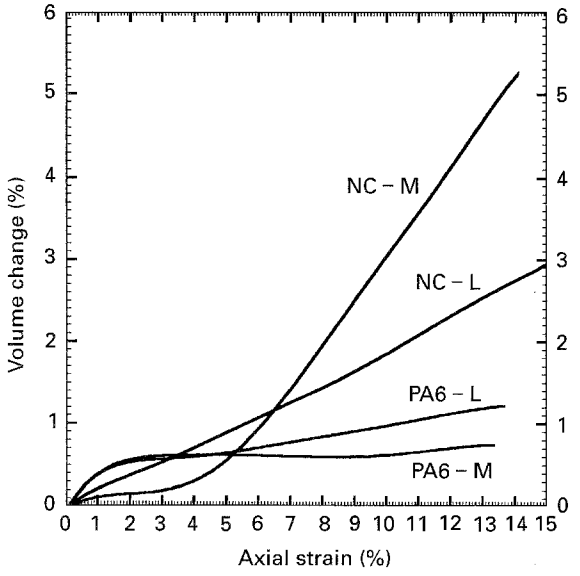

Figure 7 Volume change versus axial strain for 4 mm type II specimens. Neat PA6 and non-compatibilized (NC) are compared in the transverse (at position M) and the longitudinal (L) directions.

TABLE II Post-yield slope and Poisson's ratio, at 0.5% axial deformation for Type II specimens with 2, 4, 6 mm thickness. C, NC, with and without compatibilizer respectively. Samples were taken longitudinally (L) and transversally at position (B, M, E)

Materials	Slope	Poisson's ratio
PA-6 (M)	0.007	0.48
PA-6 (L)	0.007	0.48
2-NC (M)	0.35	0.47
2-NC (L)	0.15	0.42
4-NC (M)	0.55	0.45
4-NC (L)	0.18	0.41
6-NC (M)	0.45	0.42
6-NC (L)	0.32	0.48
4-NC (B)	0.45	0.48
4-NC (E)	0.40	0.48
4-C (M)	0.12	0.45
4-C (L)	0.15	0.40

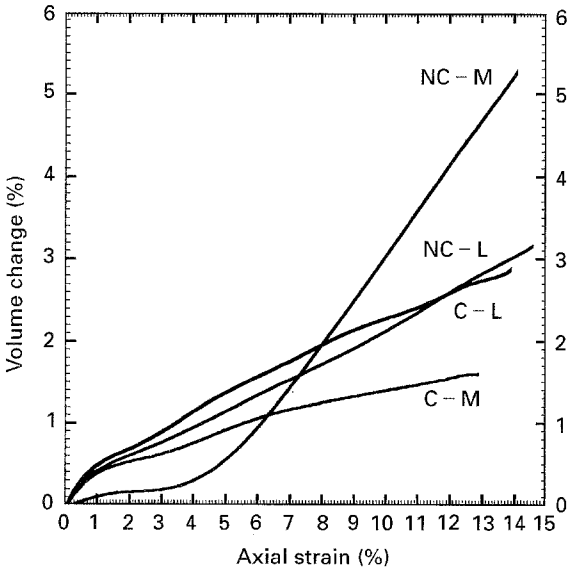

Figure 8 Volume change versus axial strain of 4 mm thick type II specimens. Compatibilized (C) and non-compatibilized (NC) samples are compared in the transverse (at position M) and the longitudinal direction (L).

3.2. Machined from plaque (type II) specimens

3.2.1. Effect of HDPE minor phase

For the case of the plaque specimen, Fig. 7 shows that in the transverse as well as in the longitudinal direction, neat PA6 deforms by pure shear yielding (a nil post-yield slope). A rapid volume increase up to 1.5% axial strain, due to the Poisson effect, is followed by a very slow volume increase suggesting isotropic properties for neat PA6. When PE is added, and after 3%–4% axial deformation which corresponds to the onset of yielding, a drastic volume increase can be observed in the transverse direction. A post-yield slope of 0.55 is obtained, indicating a mixed mechanism of deformation with 55% cavitation contribution, the remainder is due to shear yielding (Table II). The volume increase is related to the poor interface and is also due to the fact that the specimen is tested perpendicular to the direction of flow. Excessive whitening is observed. In the longitudinal direction the addition of PE causes a linear volume increase up to 2.8% at an axial strain of 15% leading to 0.18 post-yield slope, greater than for neat PA6 (slope 0.007). This may be attributed to the poor interface between the components of the blends, favouring more void formation [11].

3.2.2. Effect of interfacial modification

Fig. 8 illustrates the influence of adding a compatibilizer in a 4 mm thick sample. In the longitudinal direction the addition of a compatibilizer has little effect on the dilatometric behaviour, because the non-compatibilized sample experiences significant dispersed phase orientation and mimics the compatibilizing effect as discussed before (curves NC-L and C-L). The orientation phenomena is shown by SEM observations in Fig. 11a and b below. In the transverse direction, the effect of interfacial modification is more evident, because a drastic reduction in ΔV is observed. This supports previous findings [1, 11]; a better interface is achieved, although it can be affected by other factors such as crystallinity [30, 31]. The volume increase reaches 2% at an axial strain of 15%. The post-yield slope, as shown in Table II, changes from 0.55 for the non-compatibilized blend to 0.12 for the compatibilized one, indicating the profound effect of interfacial modification on the mechanism of deformation of such blends in the transverse direction. Poisson's ratio (Table II) is slightly increased upon addition of the compatibilizer indicating a better interface [7].

3.2.3. Effect of specimen position

The volume change versus axial deformation of non-compatibilized 4 mm thick specimens taken longitudinally (L) and transversally at positions B, M, E as shown on Fig. 1, is plotted in Fig. 9. A similar volume increase (starting at approximately 3% axial strain) can be observed for the samples cut transversally (position B, M, and E). This corresponds, as already mentioned, to the onset of yielding. Overall the effect

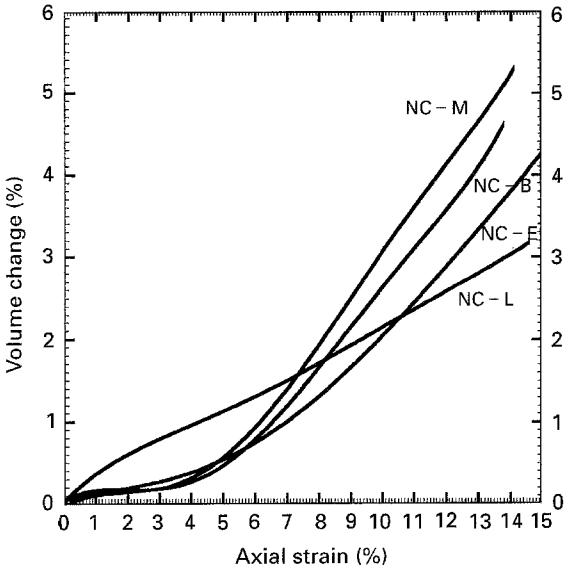

Figure 9 Volume change versus axial strain for 4 mm thick type II specimens. Non-compatibilized (NC) samples taken at positions: B, M, E, L (see Fig. 1).

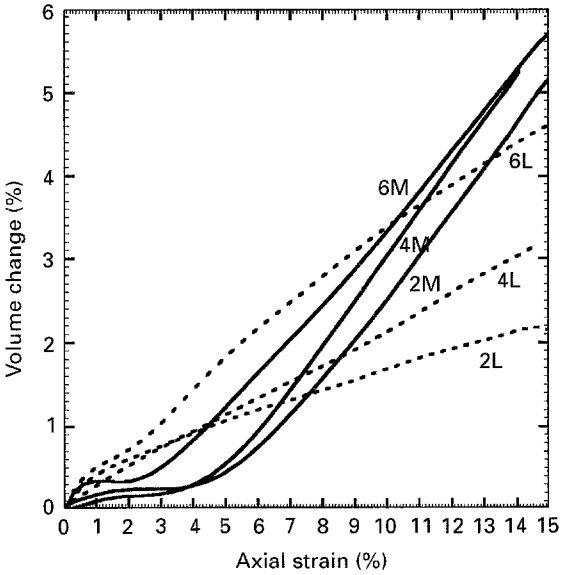

Figure 10 Volume change versus axial strain of non-compatibilized (NC) type II specimens with variable plaque thickness (2, 4, 6 mm), compared in the transverse direction (at position M) and longitudinally (L).

of position is negligible, and the dilatational properties are not highly affected (see post-yield slopes in Table II). Finally, the longitudinal specimen displays a linear volume increase (up to 3% at 15% axial deformation) right from the beginning. This can be attributed to orientation considerations. The anisotropy in the sample is clearly visible as well as the close relationship between the structure developed during processing and the resulting mechanical properties.

3.2.4. Effect of plaque thickness

The influence of plaque thickness was carried out for type II specimens with 2, 4 and 6 mm thickness, analysed transversally (at position M) and longitudinally (L). The results are illustrated in Fig. 10. Generally speaking, after yielding, the volume change in the transverse direction is significantly greater than that in the longitudinal direction (post-yield $\text{slope}_T > \text{slope}_L$ as shown in Table II). After a constant volume change up to 2%–3% axial deformation corresponding to the limit of elasticity, ΔV starts rising drastically. This is in contrast to the longitudinal direction where the ΔV is linear right from the beginning. In the transverse direction, the volume changes at a given axial strain can be classified as follows: 2 mm < 4 mm < 6 mm, although the difference with respect to specimen thickness is minimal. In the longitudinal direction, the volume difference is much more noticeable with the same order as before (2 mm < 4 mm < 6 mm). For the thick specimen, the core region is larger leading to more internal cavitation as opposed to the highly oriented skin as shown in Fig. 11. This will lead evidently to a higher volume change at a given axial strain. It appears that the skin-to-core ratio plays a major role in this case. SEM observations of samples with variable thickness concluded that the 2 mm thick specimen is composed of 150 μm core and 1850 μm skin (including subskin), the 4 mm thick sample is composed of a 2000 μm core and a 2000 μm skin (subskin included), while in the 6 mm thick sample, the core as expected is larger reaching 4000 μm leaving a skin (with subskin) of 2000 μm. The ratio of the oriented zone (skin) to the non-oriented zone (core) equals 10 for 2 mm, 1 for the 4 mm and 0.5 for the 6 mm (Fig. 11d, e). This clearly supports the previous findings that longitudinal dispersed phase orientation incurred during injection moulding plays a strong role in determining the mechanism of deformation.

3.2.5. Influence of mould type

SEM studies illustrate a skin/core ratio of 30/1 for the 3 mm dog-bone specimen (Fig. 5). For the case of the plaque (type II specimen) the skin/core ratios as discussed previously were evaluated to be 0.5/1 for 6 mm, 1/1 for 4 mm and 10/1 for 2 mm thick specimens (Fig. 11d, e). Despite these differences, very little variation is observed in the longitudinal direction during tensile dilatometry between types I and II specimens (Fig. 12). However, this study has shown that the non-compatibilized blend, analysed in the transverse direction, due to high levels of longitudinal orientation, displays significantly increased cavitation behaviour (slope of 0.55 in the transverse direction compared to 0.18 for the longitudinal one) as shown in Fig. 8 and Table II. This emphasizes the need to consider both longitudinal and transverse directions and illustrates the benefit of using plaques as opposed to directly moulded dog-bone specimens. The compatibilized blends showed little differences in their slopes (0.12 for the transverse compared to 0.15 for the longitudinal case).

The most striking results in this study indicate that the deformation mechanism in injection-moulded non-compatibilized blends is largely controlled by orientation phenomena. Tensile dilatometry experiments taken in the direction of orientation display a predominantly shear yielding process and mimic the behaviour of compatibilized systems. The importance of

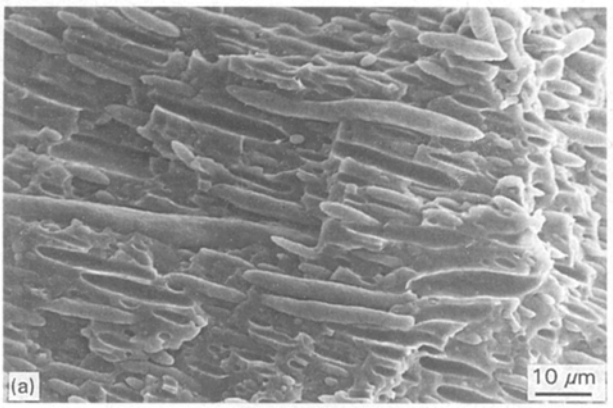

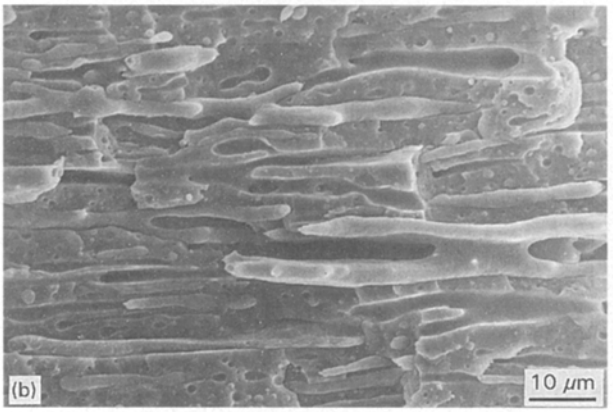

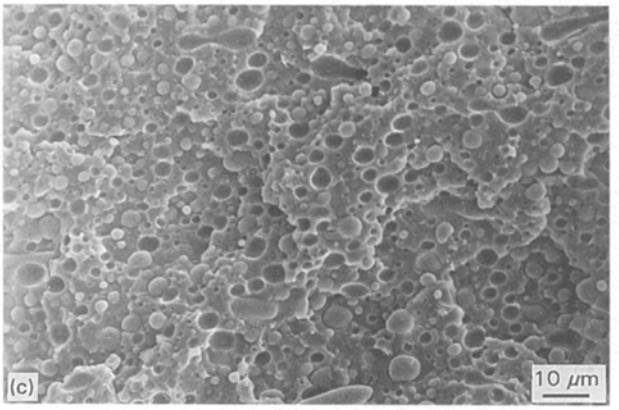

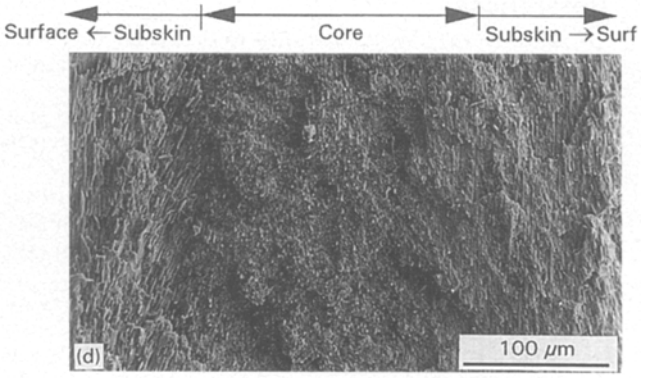

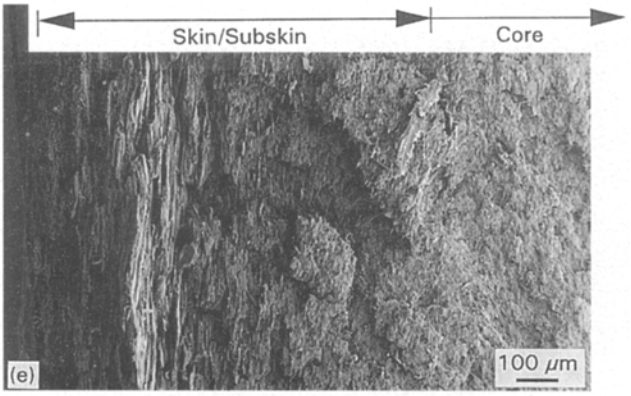

Figure 11 Non-compatibilized type II samples, (a) in the skin, (b) subskin, (c) core, all observed longitudinally. (d, e) Fracture surfaces of 2 and 4 mm thick samples observed transverse to flow.

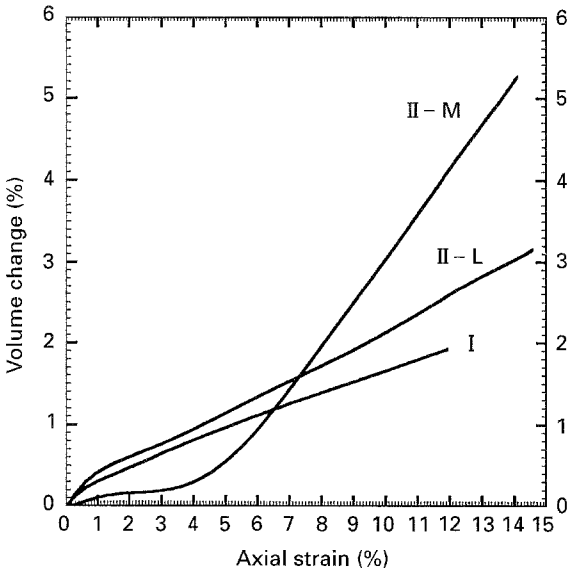

Figure 12 Volume change versus axial strain of non-compatibilized (NC) blends. Comparison between type I and type II specimens (4 mm thick), taken at positions M and L.

orientation is confirmed in studies varying the plaque thickness where the skin/core ratio is modified and also by the significant difference in longitudinal versus transverse properties. Scanning electron micrographs clearly show the significant orientation in these systems. This phenomenon appears to be principally related to the orientation of the dispersed phase because neat PA-6 behaves in an isotropic fashion.

4. Conclusion

Tensile dilatometry has been carried out for injection-moulded HDPE/PA6 blends. Directly moulded (type I) and machined from plaques (type II) tensile bars were used. In type II specimens, cut transversally to the flow direction, the addition of HDPE to PA6 dramatically transforms the deformation from essentially a pure shear yielding process to a mixed mode cavitation/shear yielding type mechanism. In type II cut longitudinally as well as type I specimens, the flow-induced orientation mimics the effect of the compatibilizer and the mechanism of deformation which prevails is almost pure shear yielding. The minor phase in the uncompatibilized blend bears its share of stress despite the debonding. This effect is even more evident when a rigid minor phase (glass beads) is substituted for HDPE where significant mechanical loss and increased cavitation is observed. The addition

of interfacially modified glass beads results in a return to a predominantly shear yielding type mechanism. The most significant result in this study demonstrates a correlation between dispersed phase orientation and dilatational phenomena. Significant orientation in the longitudinal direction appreciably reduces the extent of cavitation in the unmodified blends in these samples. In fact, the oriented but unmodified blends closely resemble the performance of interfacially modified samples. The dilatational behaviour of the samples appears to be highly dependent on the skin/core thickness ratio.

References

1. B. D. FAVIS, *Can. J. Chem. Eng.* **69** (1991) 619.
2. L. A. UTRACKI, "Polymer blends and alloys: thermodynamics and rheology" (Hanser, Munich, 1989).
3. A. PLOCHOCKI, in "Polymer blends", Vol. 1, edited by D. R. Paul and S. Newman (Academic Press, New York, 1978) Ch. 21, p. 319.
4. T. M. LIU, H. Q. XIE, A. O'CALLAGHAN, A. RUDIN and W. E. BAKER, *J. Polym. Sci. B Polym. Phys.* **31** (1993) 1347.
5. B. FISA and M. RAHMANI, *Polym. Eng. Sci.* **31** (1991) 1330.
6. B. FISA and A. MEDDAD, *ibid.*, in press.
7. J. W. COUMANS, D. HEIKENS and S. D. SJOERDSMA, *Polymer* **21** (1980) 103.
8. M. E. J. DEKKERS and D. HEIKENS, *J. Appl. Polym. Sci.* **30** (1985) 2389.
9. R. W. TRUSS and G. A. CHADWICK, *J. Mater. Sci.* **11** (1976) 111.
10. L. G. CESSNA, *Polym. Eng. Sci.* **14** (1974) 696.
11. M. C. SCHWARZ, H. KESKULLA, J. W. BARLOW and D. R. PAUL, *J. Appl. Polym. Sci.* **35** (1988) 653.
12. C. B. BUCKNALL and D. CLAYTON, *Nature* **231** (1971) 107.
13. R. J. M. BORGGREVE, R. J. GAYMANS and H. M. EICHENWALD, *Polymer* **30** (1989) 79.
14. D. S. PARKER, H. J. SUE and A. F. YEE, *ibid.* **31** (1990) 2267.
15. M. A. MAXWELL, A. F. YEE, *Polym. Eng. Sci.* **21** (1981) 205.
16. S. I. NAQUI and I. M. ROBINSON, *J. Mater. Sci.* **28** (1993) 1421.
17. S. Y. HOBBS and M. E. J. DEKKERS, *ibid.* **24** (1989) 1316.
18. I. T. BARRIE, D. R. MOORE and S. TURNER, *Plast. Rubb. Proc. Appl.* **3** (1983) 365.
19. J. M. POWERS and R. M. CADDEL, *Polym. Eng. Sci.* **12** (1972) 432.
20. D. C. LEACH and D. R. MOORE, *Composites* **16** (1985) 113.
21. S. Y. HOBBS, M. E. J. DEKKERS and V. H. WATKINSON, *J. Mater. Sci.* **23** (1988) 1219.
22. C. B. BUCKNALL and D. CLAYTON, *ibid.* **7** (1972) 202.
23. A. F. YEE and R. A. PEARSON, *ibid.* **21** (1986) 2462.
24. E. A. A. VAN HARTIGSVELDT, *PhD. thesis*, University of Delft Holland (1987).
25. H. BERTILSON, B. FRANZEN and J. KUBAT, *Plast. Rubb. Process. Appl.* (1991).
26. S. FELLAHI, B. D. FAVIS and B. FISA, *SPE Antec Tech. Papers* **39** (1993) 211.
27. *Idem, Polymer*, in press.
28. A. MEDDAD, S. FELLAHI, M. PINARD and B. FISA, *SPE Antec Tech. Papers* **40** (1994) 2284.
29. R. ARMAT and A. MOET, *Polymer* **34** (1993) 977.
30. D. W. BARTLETT, J. W. BARLOW and D. R. PAUL, *J. Appl. Polym. Sci.* **27** (1982) 235.
31. G. MENGES, A. TROOST, J. KOSKE, H. RIES and H. STABREY, *Kunstst. Germ. Plast.* **78** (1988) 22.

Received 27 May 1994
and accepted 11 April 1995